BASIC—LIVER, PANCREAS, AND BILIARY TRACT

Development of Nonalcoholic Steatohepatitis in Insulin-Resistant Liver-Specific S503A Carcinoembryonic Antigen-Related Cell Adhesion Molecule 1 Mutant Mice

SANG JUN LEE,* GARRETT HEINRICH,* LARISA FEDOROVA,‡ QUSAI Y. AL–SHARE,* KELLY J. LEDFORD,* MATS A. FERNSTROM,* MARCIA F. McINERNEY,§ SANDRA K. ERICKSON,‖ CARA GATTO–WEIS,¶ and SONIA M. NAJJAR*

*The Center for Diabetes and Endocrine Research and the Department of Physiology and Pharmacology, ‡Department of Medicine, and the ¶Department of Pathology at the College of Medicine at the University of Toledo, Health Science Campus, Toledo, Ohio; §Department of Medicinal and Biological Chemistry at the College of Pharmacy at the University of Toledo, Main Campus, Toledo, Ohio; and the ‖Department of Medicine, University of California, and Veterans Affairs Medical Center, San Francisco, California

Background & Aims: **Liver-specific inactivation of carcinoembryonic antigen–related cell adhesion molecule 1 causes hyperinsulinemia and insulin resistance, which result from impaired insulin clearance, in liver-specific S503A carcinoembryonic antigen–related cell adhesion molecule 1 mutant mice (L-SACC1). These mice also develop steatosis. Because hepatic fat accumulation precedes hepatitis, lipid peroxidation, and apoptosis in the pathogenesis of nonalcoholic steatohepatitis (NASH), we investigated whether a high-fat diet, by causing inflammation, is sufficient to induce hepatitis and other features of NASH in L-SACC1 mice.** ***Methods:*** **L-SACC1 and wild-type mice were placed on a high-fat diet for 3 months, then several biochemical and histologic analyses were performed to investigate the NASH phenotype.** ***Results:*** **A high-fat diet caused hepatic macrosteatosis and hepatitis, characterized by increased hepatic tumor necrosis factor α levels and activation of the NF-κB pathway in L-SACC1 but not in wild-type mice. The high-fat diet also induced necrosis and apoptosis in the livers of the L-SACC1 mice. Insulin resistance in L-SACC1 fed a high-fat diet increased the hepatic procollagen protein level, suggesting a role in the development of fibrosis.** ***Conclusions:*** **A high-fat diet induces key features of human NASH in insulin-resistant L-SACC1 mice, validating this model as a tool to study the molecular mechanisms of NASH.**

About one third of adults in the United States are diagnosed with fatty liver disease, with 20%–30% predicted to develop fibrosing steatohepatitis and 10% showing the full spectrum of nonalcoholic steatohepatitis (NASH). Incidence of the disease is expected to increase in parallel to the increased prevalence of obesity.[1] With NASH progressing to cirrhosis and/or hepatocellular carcinoma and causing end-stage liver disease,[2] the disease is projected to become the leading liver disease and cause of liver transplantation as a result of cirrhosis in Western countries.

NASH is characterized by hepatic macrosteatosis, inflammation, and fibrosis. Its pathogenesis is not fully elucidated, but the most prevalent mechanism is the "two-hit" hypothesis.[3] According to this hypothesis, hepatic steatosis initially develops (first hit) and predisposes to lipid peroxidation and inflammation, leading to hepatitis, apoptosis, fibrosis, and, ultimately, cirrhosis (second hit).

Activation of hepatic peroxisome proliferator-activated receptor α (PPARα)-dependent mechanisms during fasting increases transcription of enzymes involved in fatty acid mitochondrial transport and β-oxidation, such as carnitine palmitoyl transferase 1, to support gluconeogenesis. Some of these are co-regulated by PPARγ co-activator 1α (PGC-1α),[4] which is involved

mainly in promoting mitochondrial biogenesis and regulation of genes in the oxidative phosphorylation chain, such as the mitochondrial uncoupled protein-2 (UCP2), which reduces adenosine triphosphate synthesis when activated by superoxides and the lipid peroxidation end products.[5] Under conditions of obesity and prolonged high-fat intake, excessive fatty acid oxidation and lipid ω-peroxidation promote oxidative stress.[6] Together with reduction of the mitochondrial glutathione (GSH) defense system against the cytotoxic effect of tumor necrosis factor α (TNFα), this activates IκB kinase (IKK)β-dependent nuclear factor κ B (NF-κB) inflammatory pathways and causes insulin resistance,[7] hepatitis,[8] and mitochondrial dysfunction. It also predisposes to cell death and hepatocyte susceptibility to injury, and progressive liver diseases such as NASH.[9]

Although NASH may develop in association with insulin resistance,[10,11] the molecular relationship has not been well delineated,[12] in part owing to the lack of an animal model that replicates the human state adequately. No animal model has developed NASH spontaneously, and few may develop some of the clinical manifestations of the disease.[12,13] The methionine-choline–deficient diet induces fibrosing steatohepatitis. However, human beings with NASH do not show methionine or choline deficiency and this diet does not cause insulin resistance. The relevance of the leptin-deficient *Ob/Ob* obese mouse in NASH pathogenesis also has been questionable because altered leptin signaling can itself modulate inflammatory response, fibrosis, and hepatic lipid metabolism.[14] Insight provided by the phosphatase and tensin homolog on chromosome 10 mutant mouse also is limited because it is insulin sensitive and lean, and it develops massive steatosis by comparison with human NASH.[15] The transgenic mouse with adipose tissue–specific expression of nuclear sterol regulatory element-binding protein 1c (SREBP-1c) displays marked steatosis with a liver histology similar to NASH.[16] Because this mouse shows inherited lipodystrophy with hypoleptinemia and severe insulin resistance, it does not fully replicate the clinical manifestation of NASH. Thus, these experimental models failed to address adequately the role of insulin resistance in NASH pathogenesis.

L-SACC1 mice with liver-specific overexpression of the dominant-negative S503A phosphorylation-defective mutant of CEACAM1 (the CarcinoEmbryonic Antigen-related Cell Adhesion Molecule 1) develop hepatic steatosis with increased hepatic triglyceride output and visceral obesity,[17] resulting from impaired insulin clearance and hyperinsulinemia. This shows that CEACAM1 promotes hepatic insulin clearance in a phosphorylation-dependent manner. CEACAM1 also acts as a co-inhibitory receptor after T-cell activation to inhibit inflammation.[18] Because this function depends on the phosphorylation of immunoreceptor tyrosine-based inhibi-tion motifs within the cytoplasmic domain in addition to SHP1,[19] we investigated whether L-SACC1 mice develop a NASH-like phenotype under conditions known to trigger inflammation, such as prolonged high-fat (HF) intake.[20] We herein report that L-SACC1 mice show key features of obesity-related human NASH when fed HF for 3 months.

Materials and Methods

Animal Maintenance

Animals were kept in a 12-hour dark/light cycle and fed standard chow ad libitum. All procedures were approved by the Institutional Animal Care and Utilization Committee. Six-month-old genetically matched wild-type (WT) and L-SACC1 female mice were fed a standard chow (regular diet [RD]) or an HF diet (45% total calories from fat) for 3 months (Cat #D12451; Research Diets Inc, New Brunswick, NJ).

Metabolic Phenotype

After an overnight fast, mice were anesthetized with sodium pentobarbital at 11:00 am. Whole venous blood was drawn from the retro-orbital sinuses to measure fasting glucose levels using a glucometer (Accu-chek; Roche Applied Science, Indianapolis, IN), serum insulin and leptin levels by radioimmunoassays (Linco Research, St Charles, MO), serum free fatty acids (NEFA C kit; Wako, Osaka, Japan), triglyceride levels (Infinity Triglycerides; Sigma, St Louis, MO) and cholesterol levels (Pointe Scientific, Canton, MI), and free cholesterol (Wako). Serum alanine aminotransferase (ALT) and aspartate aminotransferase (AST) levels were measured per the manufacturer's instructions (Biotron Diagnostic, Hemet, CA). Visceral adipose tissue was excised, weighed, and visceral adiposity was expressed as a percentage of total body weight. Hepatic total cholesterol and free cholesterol were measured using the Infinity cholesterol reagent (Thermo Electron, Waltham, MA) and a free cholesterol reagent (Wako), respectively.[21]

Liver Histology

Histologic examination was established using H&E of formalin-fixed, paraffin-embedded liver. The degree of steatosis and lobular inflammation was graded on a 0–3 scale, with 3 being the highest, according to the NASH scoring system, which recently was proposed by the National Institute for Diabetes and Digestive and Kidney Diseases–NASH Clinical Research Network.[22]

Liver Staining

Deparaffinized and rehydrated slides were incubated in a 0.1% solution of Sirius Red (Direct Red 80; Sigma) in saturated picric acid in the dark for 1 hour and mounted with resin. For the terminal deoxynucleotidyl transferase–mediated deoxyuridine triphosphate nick-end labeling assay, sections were stained with ApopTag

Plus Peroxidase Apoptosis Detection Kit (Chemicon International, Temecula, CA) per the manufacturer's instructions. For immunohistochemical analysis, liver sections were blocked in 1.5% horse serum (Vector Laboratories, Burlingame, CA) for 30 minutes and probed with fluorescein isothiocyanate–conjugated anti-mouse antibodies to F4/80 (1:20; eBioscience, San Diego, CA), and CD3 or CD4 (1:100; BD Pharmingen, San Diego, CA) for 1 hour in the dark. Nuclei were counterstained with propidium iodide. Eight to 10 random fields per section were counted. Images were captured using a Leica TCS SP5 broadband confocal microscope (Wetzlar, Germany).

GSH Assay

Reduced glutathione was measured using the Bioxytech GSH-400 kit (OXISResearch, Portland, OR).[23] Briefly, liver tissue was homogenized in 5% metaphosphoric acid before adding a chromogenic reagent (4-chloro-1-methyl-7-trifluromethyl-quinolinium methylsulfate) and 30% NaOH, followed by incubation at room temperature for 10 minutes in the dark and measurement at A400 nm.

Nitrite Assay

Serum nitrite levels were measured using the Griess reagent system (Promega, Madison, WI). Briefly, equal amounts of sulfanilamide solution and N-1-napthylethylenediamine dihydrochloride solution were added to equal volumes of serum, and allowed to incubate at room temperature for 10 minutes before measurement at A540 nm.

Thiobarbituric Acid Reactive Substances Assay

Lipid peroxidation was measured as described[13] with modifications. Briefly, liver tissue was homogenized in 1.15% KCl before centrifugation at 10,000 rpm at 4°C for 10 minutes. The supernatant (100 μL) was added to 8.1% sodium dodecyl sulfate, 20% acetic acid, and 0.8% thiobarbituric acid, followed by heating at 95°C for 60 minutes. n-butanol-pyridine (15:1) was added to the cool mix before centrifugation at 4000 $\times$ g for 10 minutes and the upper layer was measured at A532 nm.

Western Analysis

Total tissue lysates or 10 μg serum lysates (for ApoB) were analyzed by 4%–12% gradient sodium dodecyl sulfate–polyacrylamide gel electrophoresis (Invitrogen, Carlsbad, CA) before Western analysis with polyclonal antibodies against PPARα, PGC-1α, UCP2 (Santa Cruz Biotechnology, Santa Cruz, CA), cytochrome p450 enzyme (Chemicon International), ApoB48/100 (Chemicon International), fatty acid synthase,[24] Niemann Pick type C1 (NPC-1) (Abcam, Cambridge, MA), procollagen (SouthernBiotech, Birmingham, AL), and p65 NF-κB phosphoserine (Ser 536), p65 NF-kB, and protein kinase C (PKCζ) phosphothreonine-Thr 410/403 (Cell Signaling Technology, Danvers, MA), in addition to monoclonal antibodies against PPARγ, PKCζ, glyceraldehyde-3-phosphate dehydrogenase (GAPDH) (Santa Cruz), and actin (Sigma). Membranes were incubated with horseradish-peroxidase–conjugated anti–immunoglobulin G antibody and proteins

Table 1. Phenotype Characterization of Age- and Sex-Matched WT and L-SACC1 Mice Fed an RD or HF Diet for 3 Months

	WT		SACC1	
	RD	HF	RD	HF
ALT level, μmol/L	42.4 ± 1.01	41.0 ± 1.15	54.2 ± 4.88[a]	50.3 ± 4.02[a]
AST level, μmol/L	140. ± 9.68	160. ± 6.27	185. ± 11.2[a]	170. ± 7.31[a]
Body weight, g	20.5 ± 0.66	28.3 ± 3.10[b]	27.1 ± 1.76[a]	36.4 ± 1.71[a,b]
Visceral fat, % bwt	0.18 ± 0.08	5.50 ± 2.26[b]	4.96 ± 1.33[a]	12.4 ± 2.85[a,b]
Random blood glucose level, mg/dL	67.5 ± 6.74	115. ± 9.40[b]	108. ± 5.78[a]	130. ± 7.50[a,b]
Fasting blood glucose level, mg/dL	58.3 ± 13.1	58.0 ± 4.57	45.7 ± 4.40	87.0 ± 18.2[a,b]
Serum leptin level, mg/dL	11.6 ± 1.08	33.5 ± 11.8[b]	65.6 ± 22.2[a]	98.0 ± 33.7[a]
Serum insulin, pmol/L	73.0 ± 2.55	153. ± 22.6[b]	153. ± 23.4[a]	188. ± 28.2[a]
Serum free fatty acid level, mEq/L	0.38 ± 0.01	0.52 ± 0.07[b]	0.68 ± 0.08[a]	0.74 ± 0.08[a]
Serum triglyceride level, mg/dL	40.2 ± 4.68	52.3 ± 12.4	63.4 ± 3.27[a]	27.8 ± 3.49[a,b]
Hepatic triglyceride, mg/g protein	23.6 ± 2.81	36.5 ± 3.07[b]	34.2 ± 3.41[a]	49.3 ± 3.58[a,b]
Serum cholesterol level, ng/dL	61.2 ± 1.18	72.0 ± 5.36	62.7 ± 3.04	76.1 ± 9.75
Hepatic total cholesterol, μg/mg protein	15.4 ± 1.21	15.7 ± 0.62	13.2 ± 0.51	15.8 ± 1.27
Hepatic free cholesterol, μg/mg protein	11.9 ± 0.93	10.7 ± 0.50	6.83 ± 0.65[a]	8.55 ± 0.73[a]
Hepatic cholesterol esters, μg/mg protein	3.57 ± 0.55	4.97 ± 0.62	6.36 ± 0.46[a]	7.28 ± 1.00[a]
In vivo cholesterol synthesis, μmol ^3H_2O incorporation/h/g				
Whole body	0.89 ± 0.10		0.69 ± 0.11	
Liver	4.72 ± 0.72		9.99 ± 1.28[a]	
Heart	0.10 ± 0.10		0.06 ± 0.05	
Small intestine	1.70 ± 0.16		2.07 ± 0.09	

[a]$P < .05$ vs WT-RD. Values are expressed as mean ± SEM.
[b]$P < .05$ HF vs RD. Values are expressed as mean ± SEM.

were detected by enhanced chemiluminescence (Amersham Pharmacia Biotech, Buckinghamshire, United Kingdom) and quantified by densitometry.

Northern Analysis

Liver messenger RNA (mRNA) was extracted with Trizol (Invitrogen) and the MicroPoly(A) Pure kit (Ambion, Austin, TX) before probing with Random Primed–labeled complementary DNAs (cDNAs) (Roche) for carnitine palmitoyl transferase 1, phosphoenolpyruvate carboxykinase (PEPCK), pyruvate dehydrogenate kinase (PDK-4), glucose-6-phosphatase (G-6-Pase), SREBP1c, and TNFα before reprobing with GAPDH cDNA to normalize for the amount loaded.

Real-Time Polymerase Chain Reaction

RNA was extracted using RNeasy Mini Kits (Qiagen, Valencia, CA) before TNFα cDNA was synthesized by M-MLV reverse transcriptase, and its level was quantitated by Absolute SYBR Green real-time PCR mastermix (Thermo Fisher Scientific, Waltham, MA) in a Bio-Rad I-cycler (Hercules, CA). TNFα level was normalized with GAPDH using the following primers: TNFα forward: TTCTGTCTACTGAACTTCGGGGTGATCGGTCC, TNFα reverse: GTATGAGATAGCAAATCGGCTGACGGTGTGGG, GAPDH forward: CCAGGTTGTCTCCTGCGACT, and GAPDH reverse: ATACCAGGAAATGAGCTTGACAAAGT.

Statistical Analysis

Data were analyzed with Statview software (Abacus, Berkeley, CA) using one-factor analysis of variance. A P value of less than .05 was considered statistically significant.

Results

HF Diet Exacerbates the Metabolic Derangement in L-SACC1 Mice

As previously reported,[17,25] 9-month-old female L-SACC1 mice develop higher body weight and visceral obesity by comparison with their WT counterparts (Table 1). Prolonged HF intake for 3 months increases visceral fat and, consequently, serum leptin levels, in both groups of mice,
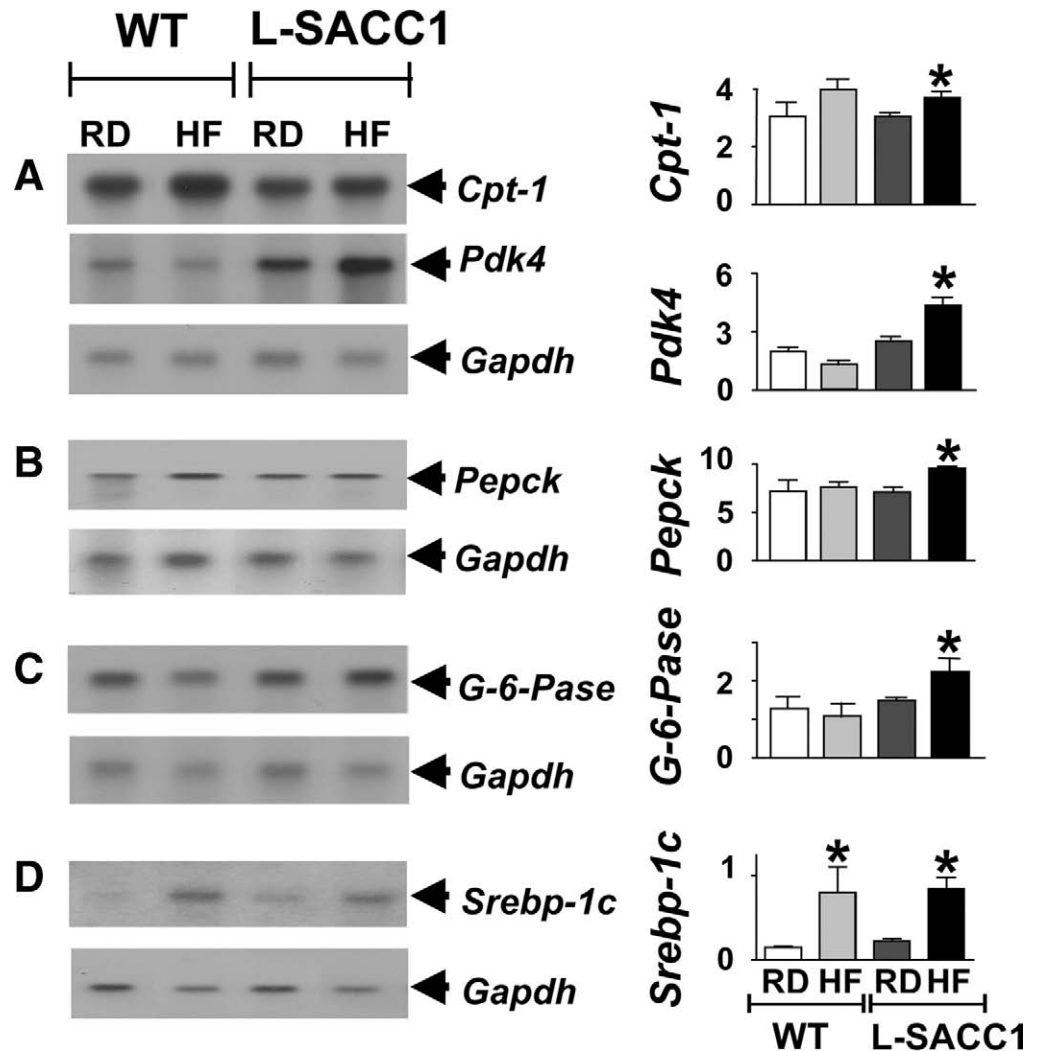

Figure 1. Northern analysis of hepatic enzymes. Liver was extracted from fed WT and L-SACC1 mice, which had been RD-fed or HF-fed for 3 months, and mRNA was purified and analyzed sequentially for (A) Cpt-1, Pdk4, and Gapdh levels. (B) Another aliquot was analyzed for *G-6-Pase* and *Gapdh* mRNA levels. (C and D) Other aliquots were analyzed for *Pepck* and *Srebp1c*, respectively, before reprobing with *Gapdh* mRNA levels. Bands were quantitated by densitometry and presented in the graph as arbitrary units. More than 5 samples were used from each feeding group of mice. Values are mean ± SE. *P < .05 HF vs RD.

with a stronger effect on WT mice (Table 1). Moreover, HF increases serum insulin and free fatty acid levels by approximately 2-fold in WT, but not L-SACC1, mice (Table 1).

Consistent with insulin resistance,[17,25] random glucose level is higher in RD-fed L-SACC1 than WT mice (Table 1). An increase in hepatic *Pepck* and *G-6-Pase* mRNA levels at fasting,[17,25] but not postprandial state, mice fed a chow-diet (RD) (Figure 1) suggests that L-SACC1 mice are geared toward gluconeogenesis, and hence are predisposed to develop fasting hyperglycemia in response to
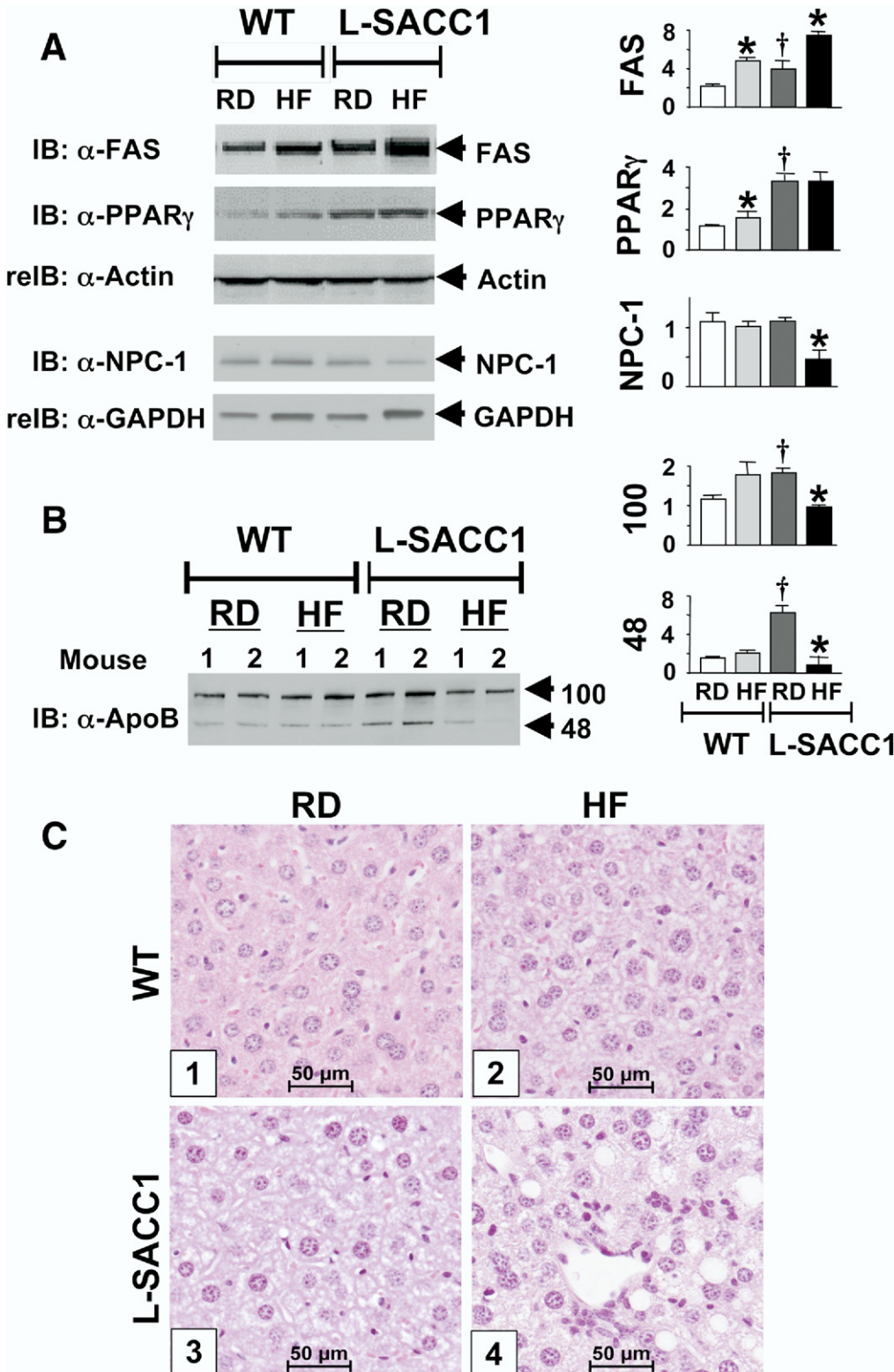

Figure 2. Hepatic lipid metabolism. (*A*) Liver lysates from more than 3 mice from each of the 4 feeding groups (RD- and HF-WT, and RD- and HF–L-SACC1) were analyzed by immunoblotting (IB) with α-fatty acid synthase (FAS), α-PPARγ, and α–NPC-1 antibodies followed by reprobing (reIB) with α-actin or α-GAPDH to normalize for the amount of protein loaded. (*B*) A total of 10 μg serum proteins from more than 5 mice per feeding group were analyzed by Western blotting with α-ApoB antibody to detect ApoB100 (~500 kilodaltons) and ApoB48 (~200 kilodaltons), which were quantitated by densitometry and presented in the bar graph as arbitrary units. Values are mean ± SE. *$P < .05$ HF vs RD. †$P < .05$ vs WT-RD. (*C*) Liver sections from more than 5 mice of each of WT-RD (*block 1*), WT-HF (*block 2*), L-SACC1–RD (*block 3*), and L-SACC1–HF (*block 4*) were analyzed by H&E staining for lipid accumulation.

the HF diet. In fact, HF causes an approximately 2-fold increase (Table 1) in the fasting glucose level of L-SACC1 mice together with a significant increase in hepatic postprandial mRNA levels of gluconeogenic enzymes: *Pepck*, *G-6-Pase*, and *Pdk-4* (Figure 1). In contrast, HF does not alter the fasting blood glucose level in WT mice. Instead, it causes a more marked increase in fed glucose level (~2-fold) than in L-SACC1 mice (Table 1).

HF Diet Alters Lipid Metabolism in L-SACC1 Mice

As previously reported,[17] hepatic triglyceride content is higher in L-SACC1 than in WT mice (Table 1), but in response to HF it is increased to the same extent (~1.8-fold) in both mouse groups (Table 1). Because hyperinsulinemia increases the transcription of lipogenic
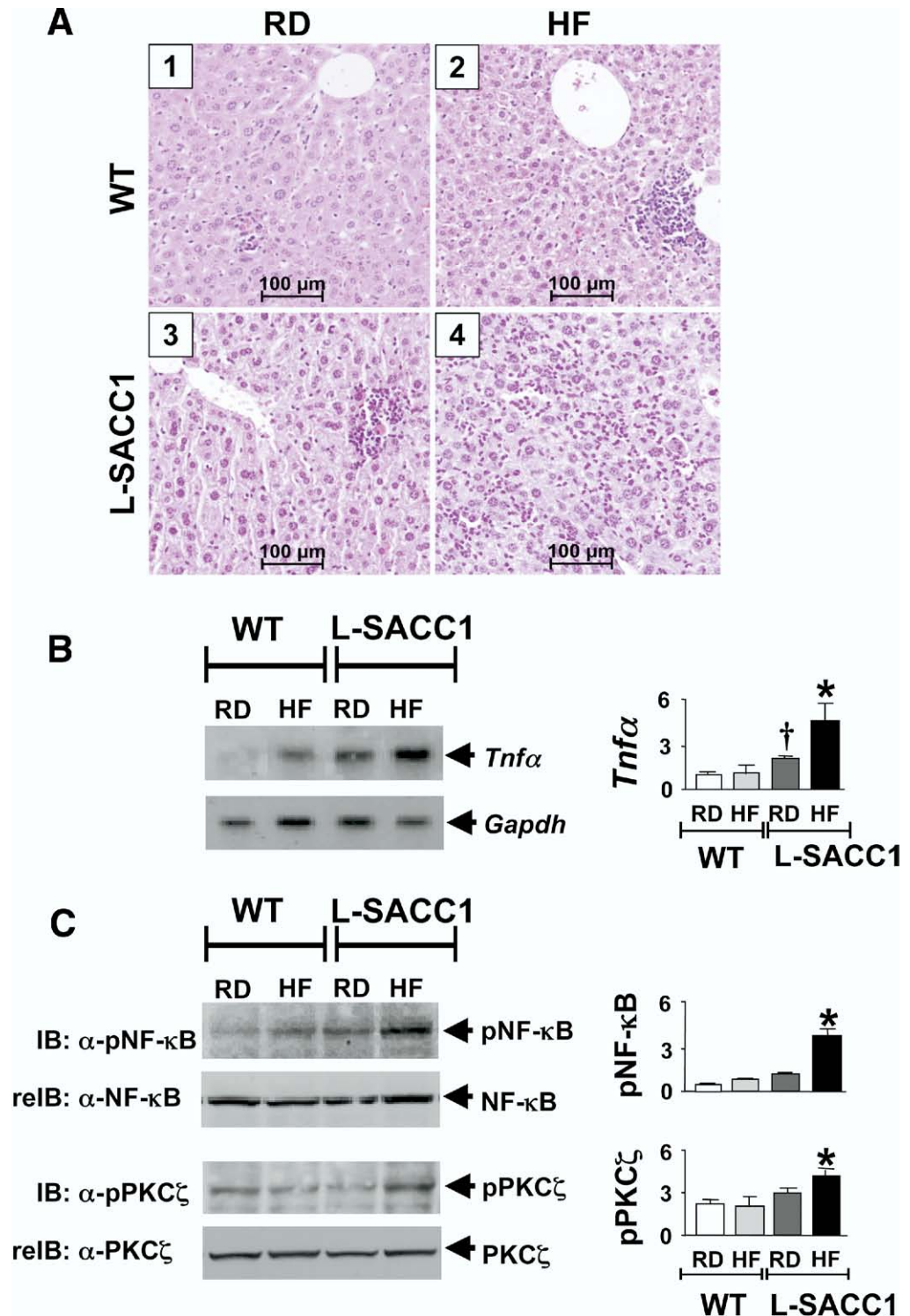

Figure 3. Characterization of hepatic inflammation. (*A*) Liver sections from more than 5 mice per feeding group were analyzed by H&E staining for inflammatory cell infiltration. (*B*) Hepatic *Tnfα* mRNA levels from more than 3 mice per feeding group were determined by Northern analysis, as in Figure 1. Values are mean ± SE. *$P <$ .05 HF vs RD. †$P <$ .05 vs WT-RD. (*C*) Liver lysates from more than 3 mice per feeding group were analyzed by Western blotting (ɪʙ) with α-phospho–NF-κB (*upper gel*) and reprobing (reɪʙ) with α–NF-κB (*lower gel*). Activation of protein kinase C (ᴘᴋᴄ)ζ was analyzed similarly for the amount of phosphorylated (*upper gel*) relative to protein level of PKCζ (*lower gel*). Bands were quantitated by densitometry and presented in the graph as arbitrary units.

enzymes,[26] this could result, at least in part, from increased de novo lipogenesis, as suggested by the approximately 2- to 3-fold increase in hepatic mRNA levels of *Srebp-1c* (Figure 1C) and the protein level of one of its targets, fatty acid synthase (Figure 2A). Basal protein expression of PPARγ, a key regulator of lipogenesis in adipocytes, is higher in L-SACC1 relative to WT livers (~3-fold) (Figure 2A; RD-fed L-SACC1 vs WT) and does not increase further by HF (Figure 2A; HF-fed vs RD-fed L-SACC1 mice). The increase in hepatic de novo lipogenesis in L-SACC1 mice correlates with higher serum triglyceride levels when mice are fed RD (Table 1), but not HF, which causes a marked decrease in serum triglyceride (Table 1) and ApoB100/ApoB48 protein levels (Figure 2B). The latter suggests reduced hepatic output of triglycerides by HF in L-SACC1 mice. In WT mice, HF does not increase serum triglyceride levels despite increasing hepatic production, as indicated by increased *Srebp-1c* (Figure 1), fatty acid synthase, and PPARγ levels (Figure 2A). With serum ApoB100/Apo48 protein content being normal (Figure 2B), a reduction in serum triglyceride could result from substrate redistribution from liver to white adipose tissue, as suggested by increased visceral obesity and increased release of free fatty acids and leptin in HF-fed WT mice (Table 1).

Although total body and intestinal in vivo cholesterol synthesis are unchanged, hepatic cholesterol synthesis is higher (~2-fold) in chow-fed L-SACC1 mice (Table 1). This leads to an increase in hepatic content of cholesterol esters with a reciprocal decrease in free cholesterol levels, resulting in a net balance of total cholesterol levels in liver and serum from L-SACC1 mice (Table 1). Although HF does not change hepatic cholesterol levels, it reduces significantly (~50%) the hepatic protein content of NPC-1, a late endosomal cholesterol traffic protein, in L-SACC1, but not WT, mice (Figure 2A).

H&E staining of liver sections reveals that HF differentially modifies the histologic manifestation of steatosis in L-SACC1 and WT mice (Figure 2C). HF markedly increases hepatic steatosis in L-SACC1 mice (score, 1.33 ± 0.28 vs 0.30 ± 0.12 in RD-fed mice; $P < .05$), and changes its histology from microsteatosis (Figure 2C, *block 3*) to macrosteatosis (Figure 2C, *block 4*). In WT mice, however, HF increases steatosis (score, 0.58 ± 0.30 vs 0.00 ± 0.00 in RD-fed mice; $P < .05$), while preserving its microvesicular histology (Figure 2C, *block 2*).

HF Diet Induces Hepatitis in L-SACC1 Mice

H&E staining of liver sections reveals that HF causes scattered inflammatory infiltration in L-SACC1 (Figure 3A, *block 4* vs *3*; score, 1.25 ± 0.28 vs 0.40 ± 0.19 in RD-fed mice; $P < .05$), with altered hepatocellular architecture. In contrast, WT mice show few, if any, inflammatory islands (Figure 3A, *block 2* vs *1*), with no significant score difference (0.42 ± 0.15 vs 0.50 ± 0.00 in RD-fed mice; $P > .05$), and maintain normal cell archi-

tecture in response to HF diet. Consistently, HF increases hepatic *Tnfα* mRNA levels (~2-fold) in L-SACC1, but not WT, mice as assessed by Northern analysis (Figure 3B). Quantitative reverse-transcription polymerase chain reaction reveals that HF diet also increases *Tnfα* mRNA levels in white adipose tissue derived from L-SACC1 mice (8.86% ± 1.42% vs 3.83% ± 0.99% *Gapdh* in RD-fed mice; $P = .023$), but not WT mice (1.54% ± 0.03% vs 1.99% ± 0.05% *Gapdh* in RD-fed mice; $P > .05$).

Consistent with a role for TNFα in activating IKK-β, a redox-sensitive kinase that up-regulates proinflammatory pathways,[27] HF markedly activates NF-κB in L-SACC1 liver, as indicated by an approximately 4-fold increase in the phosphorylation of NF-κB (Figure 3C). In contrast, HF does not activate NF-κB in WT mice to the same extent (Figure 3C). In support of PKCζ playing an important role in NF-κB activation,[28] HF increases phosphorylation (activation) of PKCζ in L-SACC1, but not WT, liver (Figure 3C).
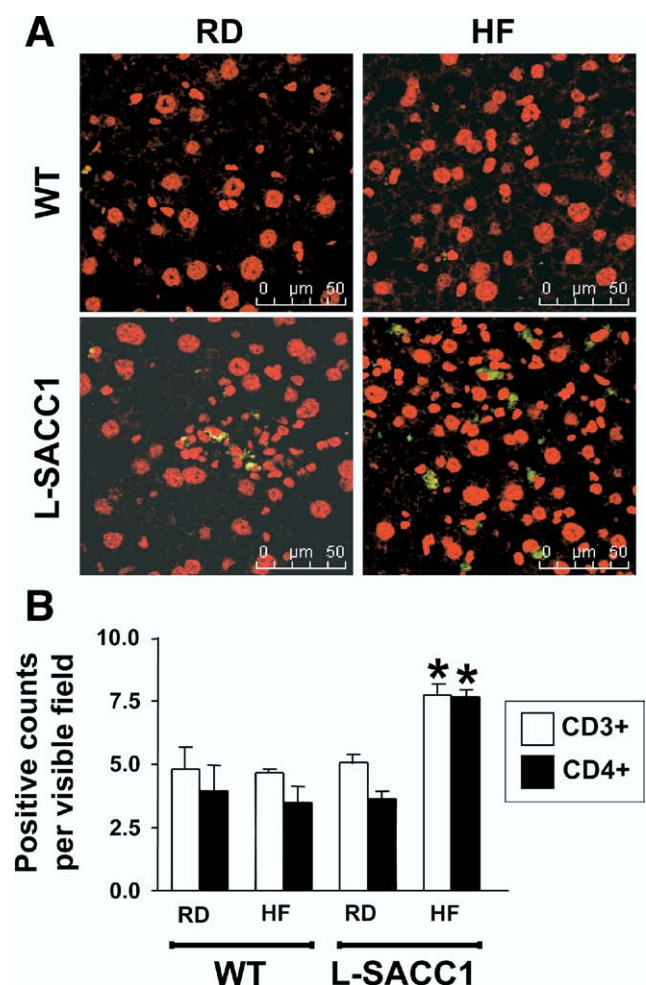

Figure 4. Immunohistochemical analysis of inflammation. Liver sections were analyzed with (A) fluorescein isothiocyanate–conjugated anti-F4/80 antibody and (B) fluorescein isothiocyanate–conjugated anti-CD3 and anti-CD4 antibodies. Experiments were repeated on 3 sections per mouse. Counts are mean positively stained cells per visible field ± SE. *$P < .05$ HF vs RD.
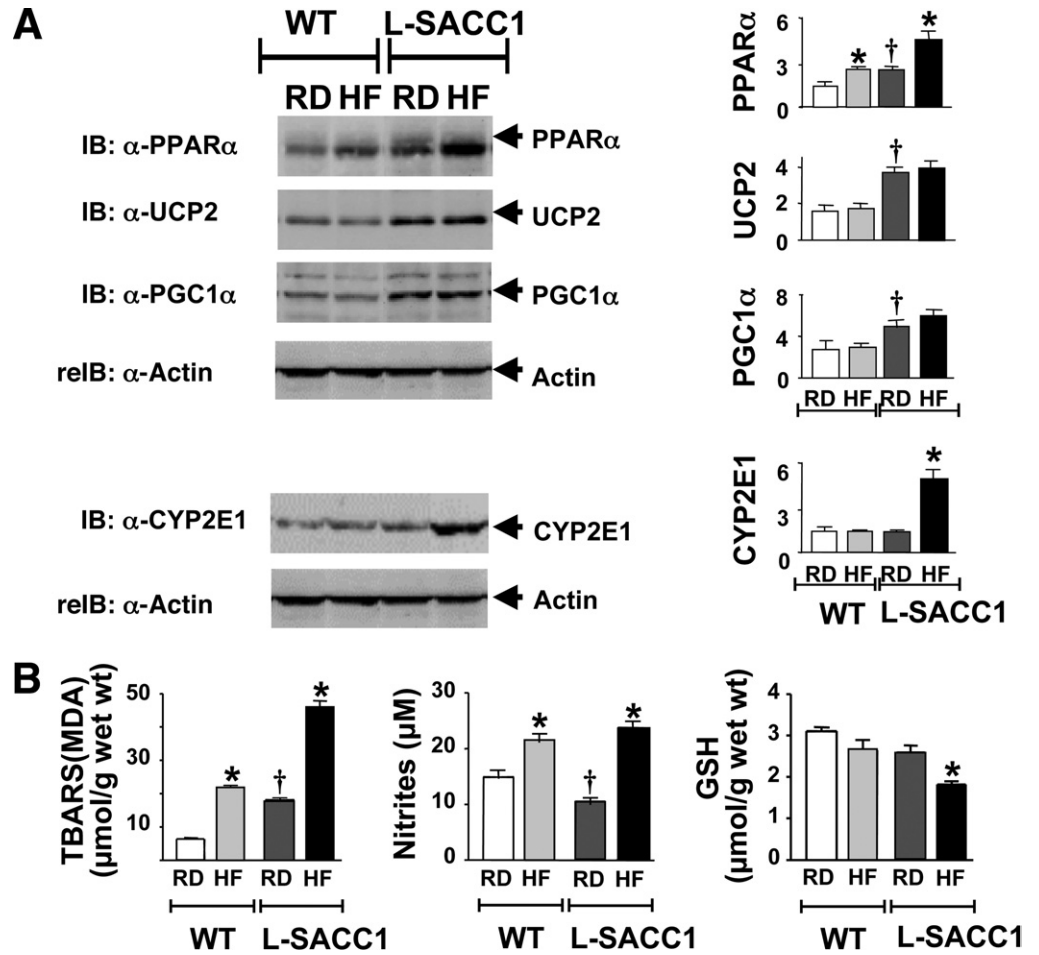
Figure 5. Nitroso-redox evaluation. (*A*) Liver lysates from more than 3 mice per feeding group were analyzed by immunoblotting (IB) sequentially with α-PPARα, α-uncoupled protein-2 (UCP2), and α-PPARγ co-activator 1α (PGC1α) antibodies before reprobing (reIB) with α-actin (*upper group of gels*). Another aliquot was analyzed similarly with α-cytochrome p450 enzyme (CYP2E1) antibody and α-actin (*lower group of gels*). Bands were quantitated by densitometry and presented in the *bar graph* as arbitrary units. (*B*) Liver (TBARS)/MDA and GSH, and serum was assayed for nitrite levels. Values are mean ± SE. *$P < .05$ HF vs RD. †$P < .05$ vs WT-RD.

In further support of increased release of TNFα from macrophages, immunostaining analysis with F4/80 reveals a larger macrophage pool in the liver of HF-fed L-SACC1 mice (Figure 4*A*, *block 4 vs 1–3, green stain*). In addition, HF induces CD3+/CD4+ T-cell population in L-SACC1, but not WT, mice as assessed by immunohistochemical analysis (Figure 4*B*). Taken together, the data indicate that HF diet induces hepatitis in L-SACC1 mice, and that this may implicate an increase in TNFα and CD4+ T-cell population, both of which are critical players in NASH pathogenesis.

HF Diet Causes Oxidative Changes in L-SACC1 Mice

Western analysis reveals that hepatic PPARα, PGC-1 1α, and UCP2 levels are higher in L-SACC1 than WT mice by approximately 2-fold (Figure 5*A*). Consistent with increased activation of PPARα by HF,[29] prolonged fat feeding induces PPARα hepatic protein levels by approximately 2-fold in both mouse groups (Figure 5*A*, *HF vs RD lanes*), and induces *Cpt1* mRNA levels with a more statistically significant effect in L-SACC1 mice (Figure 1*A*). This suggests increased fatty acid oxidation in HF-fed L-SACC1 mice.

The protein level of hepatic cytochrome p450 enzyme, a member of the microsomal cytochrome p450 that is involved in the metabolism of long-chain fatty acids (lipooxygenation) and microsomal lipid ω-peroxidation, is comparable in RD-fed L-SACC1 and WT mice (Figure 5*A*). HF increases cytochrome p450 enzyme protein level by approximately 3-fold in L-SACC1, but not WT, mice (Figure 5*A*). Moreover, lipid peroxidation, as assessed by thiobarbituric acid reactive substance concentration in liver lysates, is highly increased in HF-fed as compared with RD-fed L-SACC1 and WT mice (Figure 5*B*). This suggests initiation of oxidative changes in L-SACC1 liver by HF diet.[30] In support of this hypothesis, the level of serum nitrite, a nitric oxide oxidation product, is decreased in L-SACC1, as compared with WT mice (Figure 5*B*), suggesting lower nitric oxide bioavailability in these mice, as in other models of obesity.[31] Consistent with the positive effect of TNFα on nitrite production,[32] HF induces a more marked increase in serum nitrite level in L-SACC1 than WT mice (Figure 5*B*, HF vs RD) and decreases hepatic GSH levels in L-SACC1, but not WT, mice (Figure 5*B*). Thus, HF promotes a nitroso-redox imbalance in L-SACC1 mice.
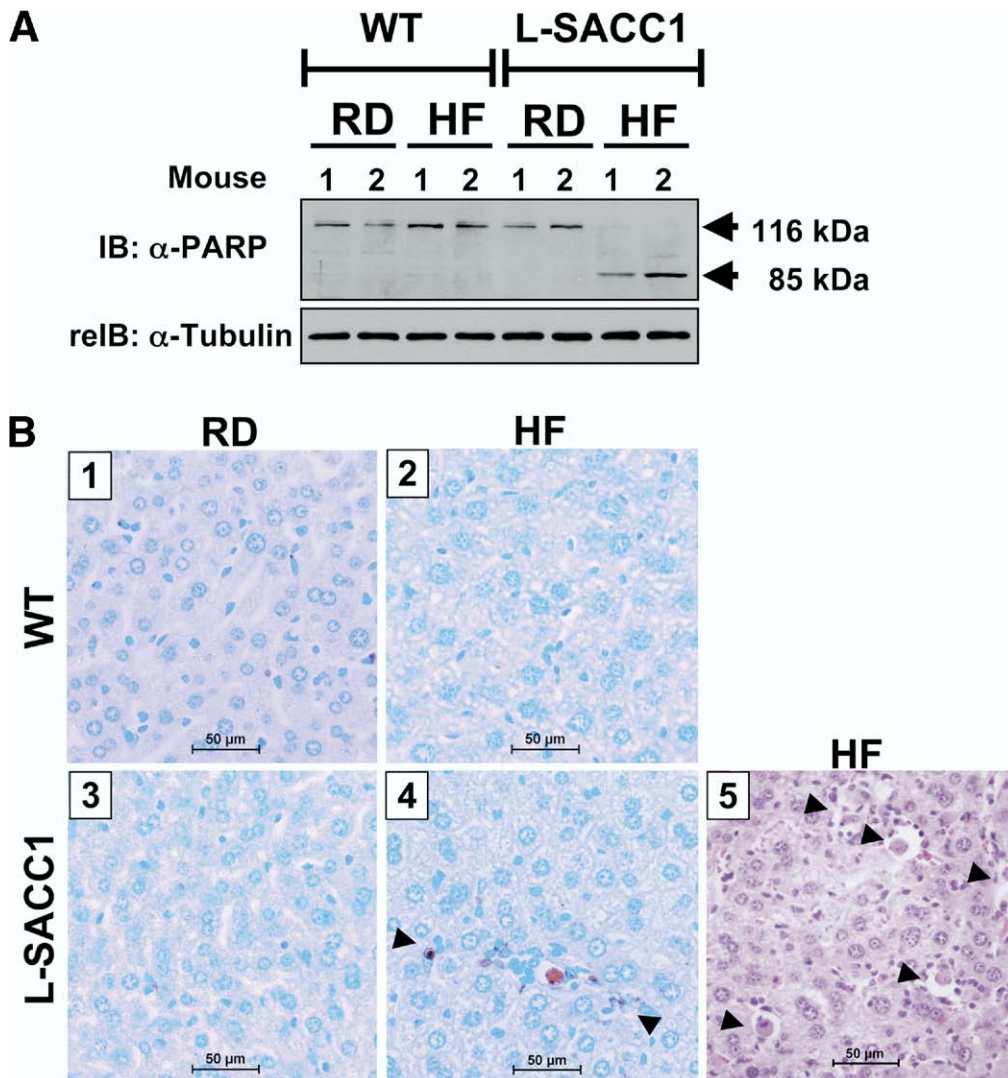
Figure 6. Analysis of cell injury. (*A*) Liver lysates from more than 5 mice were analyzed by immunoblotting (IB) with α-poly-(adenosine diphosphate-ribose) polymerase (PARP) before reprobing with α-tubulin. (*B*) Liver sections from all 4 feeding groups were analyzed by terminal deoxynucleotidyl transferase–mediated deoxyuridine triphosphate nick-end labeling (*blocks 1–4*) and H&E staining (*block 5*). Injured cells are emphasized by *arrowheads* (*blocks 4 and 5*).

HF Diet Induces Necrosis and Apoptosis in L-SACC1 Mice

Western analysis of liver lysates indicates that poly-(adenosine diphosphate-ribose) polymerase is cleaved into its smaller 85-kilodalton subunit only in HF-fed L-SACC1 mice, but not in the other groups (Figure 6A). This suggests that early apoptosis develops in L-SACC1 mice only after HF feeding.[33] This observation is supported by terminal deoxynucleotidyl transferase–mediated deoxyuridine triphosphate nick-end labeling staining, which detects histologic changes only in HF-fed L-SACC1 mice (Figure 6B, *block 4* [*arrowheads*] vs *blocks 1–3*). H&E staining reveals that livers from HF-fed L-SACC1 mice, but not others, also show necrosis (Figure 6B, *block 5* [*arrowheads*] and Figure 3, *block 4*).

Development of Early Fibrosis in L-SACC1 Mice

Liver lysates from L-SACC1 mice show increased basal procollagen protein content (Figure 7A, RD-fed

L-SACC1 vs WT), with a NASH-like chicken-wire pattern of the Sirius red stain (Figure 7B, *block 3*). In addition to inducing procollagen content (Figure 7A), HF increases chicken-wire fibrogenic changes in L-SACC1, but not WT, mice (Figure 7B, *block 4* vs *3*).

Discussion

The mechanisms underlying NASH and the role of insulin resistance in its pathogenesis are poorly understood, in part because of the lack of an experimental model replicating the full spectrum of the disease.[12] We show that L-SACC1 mice, which show insulin resistance, visceral obesity, and hepatic steatosis,[17] also develop early hepatic fibrosis together with a mild increase in serum ALT and AST levels (Table 1), and hepatic TNFα levels. When fed HF, they develop other key features of NASH, including macrosteatosis followed by hepatitis, lipid peroxidation, oxidative stress, and hepatocellular injury.

As in human NASH,[11] HF induces hepatic fatty acid oxidation and gluconeogenesis in L-SACC1 mice and
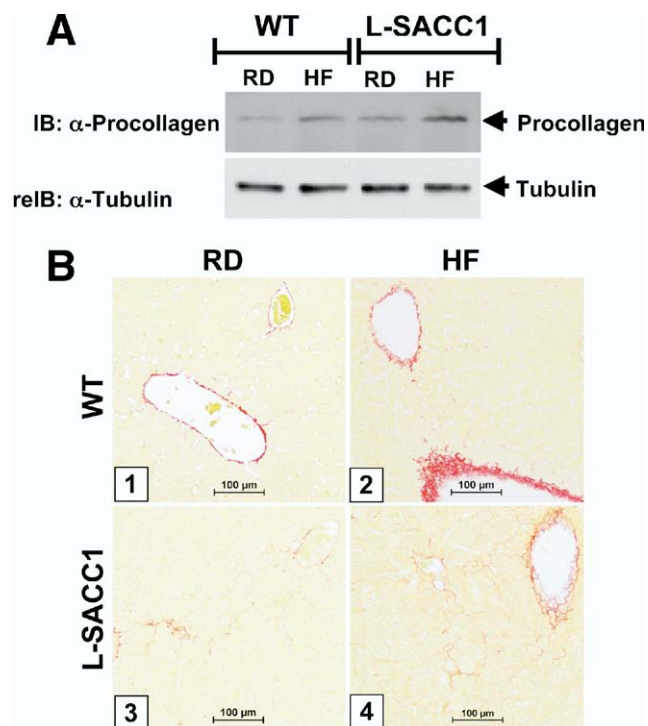
Figure 7. Analysis of fibrosis. (*A*) Liver lysates from more than 3 mice were analyzed by immunoblotting (IB) with α-procollagen antibody before reprobing (reIB) with α-tubulin. (*B*) Liver sections from more than 5 mice of each feeding group were analyzed by Sirius red staining.

causes fasting hyperglycemia. The increase in fatty acid oxidation fails to decrease hepatic triglyceride content, owing to increased triglyceride production and decreased secretion, as indicated by an increase of *Srebp-1c* mRNA and a reduction of ApoB100 levels,[34] respectively.

CEACAM1 mutation elevates hepatic cholesterol synthesis and esterification in the endoplasmic reticulum, which could be facilitated by an increased supply of de novo synthesized fatty acids in the absence of CEACAM1.[24] It is possible that the elevation in esterification occurs to prevent an increase in free cholesterol level and protect against its cytotoxic effect.[35,36] This assigns a role to CEACAM1 in integrating cholesterol metabolism and fatty acid synthetic pathways.

It is unlikely that an increase in cholesterol ester plays a role in the progression to steatohepatitis because this appears to require accumulation of free cholesterol in mitochondria.[37] We did not measure mitochondrial free cholesterol content, but reduced NPC-1 levels may partition it from cytosolic lipid droplets to mitochondria[38] in HF-fed L-SACC1 mice. As suggested by null mutation of *NPC1*,[37] this could deplete mitochondrial GSH stores and increase sensitivity to the cytotoxic effect of the proinflammatory cytokine, TNFα, the level of which is increased in these mice.

An increase in hepatic *Tnfα* mRNA could result from elevation in the pool of resident macrophages in response to increased free fatty acid supply[39] and excessive lipid accumulation in the hepatocyte, which could induce a local inflammatory response in HF-fed L-SACC1 mice.[40] It is possible that the intrahepatic inflammatory milieu is modulated by the release of adipokines, as suggested by increased *Tnfα* mRNA in visceral white adipose tissue of L-SACC1, but not WT, mice.

In agreement with experimental animal models[13,41] and human beings[42,43] with metabolic derangement, lipid peroxidation also is increased in HF-fed L-SACC1. Together with a more marked increase in serum nitrite levels, this suggests that HF causes nitroso-redox imbalance and oxidative stress, which may pave the way for peroxidative events associated with necrotic damage[44] and apoptosis[45] in L-SACC1 mice. We propose that HF causes these pathologies in L-SACC1, not WT, mice by inducing hepatic TNFα[46] and increasing sensitivity to its cytotoxic effect through alterations of the GSH-based mitochondrial defense system. Consistent with a role for TNFα-dependent activation of IKK-β in oxidative stress and inflammation of NASH,[39] HF activates NF-κB pathways to a larger extent in L-SACC1 than WT mice.

Steatohepatitis involves a Th1 cytokine response, characterized by increased cytokine release from intrahepatic CD4+ T cells.[20,47,48] Although the activation state of these cells was not examined, we observed an increase in their population in L-SACC1 mice, as has been reported for *Ob/Ob* mice.[40] Because CEACAM1 has been implicated in the anti-inflammatory response to T-cell activation,[18] it is possible that inactivating CEACAM1 in hepatocytes limits the CEACAM1-dependent inhibitory responses in T lymphocytes and leads to a robust inflammatory response to cytokines in L-SACC1 mice.

Chow-fed L-SACC1 mice show insulin resistance and hepatic steatosis. Based on the normal physiology of insulin action, one would predict that insulin resistance would not be associated with increased hepatic triglyceride content. This prediction is borne out in the LIRKO mouse.[49] However, unlike LIRKO, L-SACC1 mice have reduced, but not absent, insulin-receptor signaling, which may lead to the peculiar admixture of insulin sensitivity (in the context of increased lipogenesis) and resistance (in terms of increased fatty acid oxidation and altered glucose homeostasis) that is characteristic of NASH.

In support of the hypothesis that insulin resistance is an independent predictor for fibrosis in NASH,[50] chow-fed L-SACC1 mice develop NASH-like fibrogenic changes that can be attributed to the increase in both TNFα and leptin.[46] In fact, increased leptin levels do not play a direct role in the pathogenesis of NASH,[51] but can exacerbate the effects of TNFα.[52] In addition, L-SACC1 mice show basal mild increases in AST and ALT levels. Consistent with observations in a rabbit model of steatohepatitis,[13] HF intake does not further increase AST and ALT levels. With the majority of NASH patients showing normal AST levels,[53] this suggests that altered AST levels in

L-SACC1 mice may closely parallel the mildly increased levels in basal TNFα, leptin, and fibrogenic changes, which in turn are likely to be associated with visceral obesity, insulin resistance, and hepatic steatosis. We propose that these cellular, metabolic, and fibrogenic changes precondition the mice to develop the overt NASH phenotype in parallel to increased inflammatory activation and oxidative stress when cued by an increase in the cytotoxic effects of TNFα in response to the HF diet.

The insulin-resistant L-SACC1 mice are predisposed to developing NASH in response to HF. This could be owing to altered lipid metabolism, which leads to reduced hepatic GSH-based defense against TNFα, and to increased inflammatory response to TNFα in the absence of the anti-inflammatory effect of CEACAM1. By showing a dual role for CEACAM1 in inhibiting inflammatory response and reducing steatosis in liver, our observations indicate that a reduction in CEACAM1 may serve as a molecular link between insulin resistance and NASH.

References

1. Farrell GC, Larter CZ. Nonalcoholic fatty liver disease: from steatosis to cirrhosis. Hepatology 2006;43:S99–S112.
2. Hui JM, Kench JG, Chitturi S, et al. Long-term outcomes of cirrhosis in nonalcoholic steatohepatitis compared with hepatitis C. Hepatology 2003;38:420–427.
3. Day CP, James OF. Steatohepatitis: a tale of two "hits"? Gastroenterology 1998;114:842–845.
4. Yoon JC, Puigserver P, Chen G, et al. Control of hepatic gluconeogenesis through the transcriptional coactivator PGC-1. Nature 2001;413:131–138.
5. Echtay KS, Murphy MP, Smith RA, et al. Superoxide activates mitochondrial uncoupling protein 2 from the matrix side. Studies using targeted antioxidants. J Biol Chem 2002;277:47129–47135.
6. Chavin KD, Yang S, Lin HZ, et al. Obesity induces expression of uncoupling protein-2 in hepatocytes and promotes liver ATP depletion. J Biol Chem 1999;274:5692–5700.
7. Arkan MC, Hevener AL, Greten FR, et al. IKK-beta links inflammation to obesity-induced insulin resistance. Nat Med 2005;11:191–198.
8. Dela Pena A, Leclercq I, Field J, et al. NF-kappaB activation, rather than TNF, mediates hepatic inflammation in a murine dietary model of steatohepatitis. Gastroenterology 2005;129:1663–1674.
9. McClain CJ, Mokshagundam SP, Barve SS, et al. Mechanisms of non-alcoholic steatohepatitis. Alcohol 2004;34:67–79.
10. Marchesini G, Marzocchi R. Metabolic syndrome and NASH. Clin Liver Dis 2007;11:105–117.
11. Abdelmalek MF, Diehl AM. Nonalcoholic fatty liver disease as a complication of insulin resistance. Med Clin North Am 2007;91:1125–1149, ix.
12. Green RM. NASH—hepatic metabolism and not simply the metabolic syndrome. Hepatology 2003;38:14–17.
13. Otogawa K, Kinoshita K, Fujii H, et al. Erythrophagocytosis by liver macrophages (Kupffer cells) promotes oxidative stress, inflammation, and fibrosis in a rabbit model of steatohepatitis: implications for the pathogenesis of human nonalcoholic steatohepatitis. Am J Pathol 2007;170:967–980.
14. Leclercq IA, Farrell GC, Schriemer R, et al. Leptin is essential for the hepatic fibrogenic response to chronic liver injury. J Hepatol 2002;37:206–213.
15. Kurlawalla-Martinez C, Stiles B, Wang Y, et al. Insulin hypersensitivity and resistance to streptozotocin-induced diabetes in mice lacking PTEN in adipose tissue. Mol Cell Biol 2005;25:2498–2510.
16. Nakayama H, Otabe S, Ueno T, et al. Transgenic mice expressing nuclear sterol regulatory element-binding protein 1c in adipose tissue exhibit liver histology similar to nonalcoholic steatohepatitis. Metabolism 2007;56:470–475.
17. Poy MN, Yang Y, Rezaei K, et al. CEACAM1 regulates insulin clearance in liver. Nat Genet 2002;30:270–276.
18. Gray-Owen SD, Blumberg RS. CEACAM1: contact-dependent control of immunity. Nat Rev Immunol 2006;6:433–446.
19. Nagaishi T, Pao L, Lin SH, et al. SHP1 phosphatase-dependent T cell inhibition by CEACAM1 adhesion molecule isoforms. Immunity 2006;25:769–781.
20. Li Z, Soloski MJ, Diehl AM. Dietary factors alter hepatic innate immune system in mice with nonalcoholic fatty liver disease. Hepatology 2005;42:880–885.
21. Erickson SK, Lear SR, Dean S, et al. Hypercholesterolemia and changes in lipid and bile acid metabolism in male and female cyp7A1-deficient mice. J Lipid Res 2003;44:1001–1009.
22. Bondini S, Kleiner DE, Goodman ZD, et al. Pathologic assessment of non-alcoholic fatty liver disease. Clin Liver Dis 2007;11:17–23.
23. Kellogg AP, Wiggin TD, Larkin DD, et al. Protective effects of cyclooxygenase-2 gene inactivation against peripheral nerve dysfunction and intraepidermal nerve fiber loss in experimental diabetes. Diabetes 2007;56:2997–3005.
24. Najjar SM, Yang Y, Fernstrom MA, et al. Insulin acutely decreases hepatic fatty acid synthase activity. Cell Metab 2005;2:43–53.
25. Dai T, Abou-Rjaily GA, Al-Share' QY, et al. Interaction between altered insulin and lipid metabolism in CEACAM1-inactive transgenic mice. J Biol Chem 2004;279:45155–45161.
26. Horton JD, Goldstein JL, Brown MS. SREBPs: activators of the complete program of cholesterol and fatty acid synthesis in the liver. J Clin Invest 2002;109:1125–1131.
27. Cai D, Yuan M, Frantz DF, et al. Local and systemic insulin resistance resulting from hepatic activation of IKK-beta and NF-kappaB. Nat Med 2005;11:183–190.
28. Manicassamy S, Gupta S, Huang Z, et al. Protein kinase C-theta-mediated signals enhance CD4+T cell survival by up-regulating Bcl-xL. J Immunol 2006;176:6709–6716.
29. Patsouris D, Reddy JK, Muller M, et al. Peroxisome proliferator-activated receptor alpha mediates the effects of high-fat diet on hepatic gene expression. Endocrinology 2006;147:1508–1516.
30. Robertson G, Leclercq I, Farrell GC. Nonalcoholic steatosis and steatohepatitis. II. Cytochrome P-450 enzymes and oxidative stress. Am J Physiol Gastrointest Liver Physiol 2001;281:G1135–G1139.
31. Saraiva RM, Minhas KM, Zheng M, et al. Reduced neuronal nitric oxide synthase expression contributes to cardiac oxidative stress and nitroso-redox imbalance in ob/ob mice. Nitric Oxide 2007;16:331–338.
32. Alloatti G, Penna C, De Martino A, et al. Role of nitric oxide and platelet-activating factor in cardiac alterations induced by tumor necrosis factor-alpha in the guinea-pig papillary muscle. Cardiovasc Res 1999;41:611–619.
33. Simbulan-Rosenthal CM, Rosenthal DS, Iyer S, et al. Transient poly(ADP-ribosyl)ation of nuclear proteins and role of poly(ADP-ribose) polymerase in the early stages of apoptosis. J Biol Chem 1998;273:13703–13712.
34. Charlton M, Sreekumar R, Rasmussen D, et al. Apolipoprotein synthesis in nonalcoholic steatohepatitis. Hepatology 2002;35:898–904.
35. Tabas I. Consequences of cellular cholesterol accumulation: basic concepts and physiological implications. J Clin Invest 2002;110:905–911.

36. Soccio RE, Breslow JL. Intracellular cholesterol transport. Arterioscler Thromb Vasc Biol 2004;24:1150–1160.

37. Mari M, Caballero F, Colell A, et al. Mitochondrial free cholesterol loading sensitizes to TNF- and Fas-mediated steatohepatitis. Cell Metab 2006;4:185–198.

38. Shen WJ, Patel S, Natu V, et al. Interaction of hormone-sensitive lipase with steroidogenic acute regulatory protein: facilitation of cholesterol transfer in adrenal. J Biol Chem 2003;278:43870–43876.

39. Crespo J, Cayon A, Fernandez-Gil P, et al. Gene expression of tumor necrosis factor alpha and TNF-receptors, p55 and p75, in nonalcoholic steatohepatitis patients. Hepatology 2001;34: 1158–1163.

40. Bigorgne AE, Bouchet-Delbos L, Naveau S, et al. Obesity-induced lymphocyte hyperresponsiveness to chemokines: a new mechanism of fatty liver inflammation in obese mice. Gastroenterology 2008;134:1459–1469.

41. Enriquez A, Leclercq I, Farrell GC, et al. Altered expression of hepatic CYP2E1 and CYP4A in obese, diabetic ob/ob mice, and fa/fa Zucker rats. Biochem Biophys Res Commun 1999;255: 300–306.

42. Emery MG, Fisher JM, Chien JY, et al. CYP2E1 activity before and after weight loss in morbidly obese subjects with nonalcoholic fatty liver disease. Hepatology 2003;38:428–435.

43. Lieber CS. CYP2E1: from ASH to NASH. Hepatol Res 2004;28: 1–11.

44. Schulze-Osthoff K, Beyaert R, Vandevoorde V, et al. Depletion of the mitochondrial electron transport abrogates the cytotoxic and gene-inductive effects of TNF. EMBO J 1993;12:3095–3104.

45. Shimizu S, Eguchi Y, Kamiike W, et al. Involvement of ICE family proteases in apoptosis induced by reoxygenation of hypoxic hepatocytes. Am J Physiol 1996;271:G949–G958.

46. Carter-Kent C, Zein NN, Feldstein AE. Cytokines in the pathogenesis of fatty liver and disease progression to steatohepatitis: implications for treatment. Am J Gastroenterol 2008;103:1036–1042.

47. Kremer M, Hines IN, Milton RJ, et al. Favored T helper 1 response in a mouse model of hepatosteatosis is associated with enhanced T cell-mediated hepatitis. Hepatology 2006;44: 216–227.

48. Tiegs G. Cellular and cytokine-mediated mechanisms of inflammation and its modulation in immune-mediated liver injury. Z Gastroenterol 2007;45:63–70.

49. Biddinger SB, Hernandez-Ono A, Rask-Madsen C, et al. Hepatic insulin resistance is sufficient to produce dyslipidemia and susceptibility to atherosclerosis. Cell Metab 2008;7:125–134.

50. Angulo P, Keach JC, Batts KP, et al. Independent predictors of liver fibrosis in patients with nonalcoholic steatohepatitis. Hepatology 1999;30:1356–1362.

51. Chalasani N, Crabb DW, Cummings OW, et al. Does leptin play a role in the pathogenesis of human nonalcoholic steatohepatitis? Am J Gastroenterol 2003;98:2771–2776.

52. Manco M, Marcellini M, Giannone G, et al. Correlation of serum TNF-alpha levels and histologic liver injury scores in pediatric nonalcoholic fatty liver disease. Am J Clin Pathol 2007;127: 954–960.

53. Ong JP, Elariny H, Collantes R, et al. Predictors of nonalcoholic steatohepatitis and advanced fibrosis in morbidly obese patients. Obes Surg 2005;15:310–315.